

# Paramagnetism of Aqueous Actinide Cations. Part I: Perchloric Acid Media

Thomas F. Wall,<sup>\*,†</sup> Steve Jan,<sup>‡</sup> Matthieu Autillo,<sup>‡</sup> Kenneth L. Nash,<sup>†</sup> Laetitia Guerin,<sup>‡</sup> Claire Le Naour,<sup>¶</sup> Philippe Moisy,<sup>§</sup> and Claude Berthon<sup>\*,‡</sup>

<sup>†</sup>Department of Chemistry, Washington State University, Pullman, Washington 99163, United States

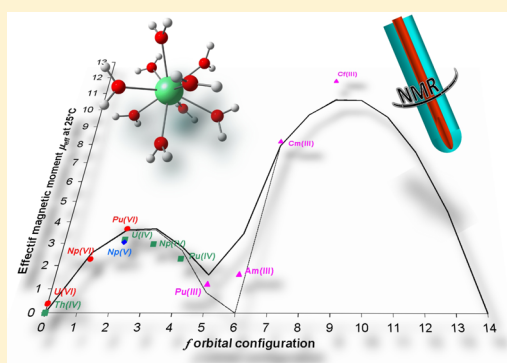
<sup>‡</sup>Nuclear Energy Division, RadioChemistry & Processes Department, Modelisation and Chemistry of Separation Processes Service, Ligand Actinide Interaction Laboratory, CEA, F-30207 Bagnols-sur-Cèze, France

<sup>¶</sup>IPN Orsay, University Paris XI, rue Georges Clemenceau, 91406 Orsay CEDEX, France

<sup>§</sup>Nuclear Energy Division, RadioChemistry & Processes Department, CEA, F-30207 Bagnols-sur-Cèze, France

## S Supporting Information

**ABSTRACT:** A comprehensive study of actinide cation paramagnetism in acidic aqueous solution has been completed in perchlorate media. Employing the Evans method, all the readily accessible actinide cations have been studied using our specially outfitted NMR spectrometer equipped for use with radioactive samples. The effective magnetic moments observed, ranging from 0 to 13  $\mu_B$ , differ from the isoelectronic lanthanides, previous solid actinide studies, and older solution studies. Actinide (IV) and (V) ions show less paramagnetic character, while some actinide (III) ions exhibit greater paramagnetic behavior than predicted from free-ion calculation. Temperature dependence of actinide magnetic susceptibilities from 5 to 80 °C are in good agreement with a Curie-like law except for U(VI), which appears to be temperature-independent. Diamagnetic behavior of Th(IV) exhibits a very low temperature dependence of the magnetic susceptibility. Some explanations for the observations are offered, and the 5f electron behavior is compared to the 4f analogues.



and the 5f electron behavior is compared to the 4f analogues.

## INTRODUCTION

Nuclear magnetic resonance spectroscopy offers considerable insights into fundamental characteristics of nuclei. It has been applied to the lanthanide elements to probe hydration sphere sizes, ordering, relaxation times, and aggregation states for both noncomplexed and bound cations.<sup>1,2</sup> Lanthanides, which exhibit paramagnetism arising from partially filled electron orbitals, are especially well-suited to analytical NMR techniques for determination of hydration sphere size<sup>3–5</sup> and Swift–Connick kinetics measurements.<sup>6–8</sup> With their ubiquitous trivalent oxidation state and partially filled f orbitals, lanthanide cations are the ideal candidates for investigation by such techniques. It follows that the extension of these techniques to actinides is a next logical step. Such an extension, particularly of coordination compounds relevant to separations, could provide valuable insight into nuclear fuel reprocessing systems. However, some of our recent attempts<sup>9</sup> at extending these techniques have been confounded by the unexpected observation of significant deviations between trivalent lanthanide and trivalent actinide behavior. For example, we have noted that the observed paramagnetism exhibited by Pu(III) in solution is weak compared to its Ln(III) analog, with no significant effect on solvent relaxation time and no discernible paramagnetically induced shifts, even at relatively high

concentrations. This contrasts strongly with the paramagnetic lanthanide (III) ions, where a relaxation time effect is observed and an induced shift is always present. These differences hint at different solution behavior and possible differences in modes of bonding interaction between the 4f and 5f series.

Considering these effects, it seemed prudent and practical to undertake a comprehensive fundamental examination of actinide paramagnetism as it relates to NMR applications. The paramagnetism of actinide solids, often expressed in Knight Shifts,<sup>10</sup> has been the subject of several investigations.<sup>11–16</sup> Initial investigations focused on the light actinide compounds (actinium through americium). Various ionic compounds of heavier members of the series (curium through einsteinium) have since been studied. However, work in the solution state is limited and dated, having been performed at the dawn of the actinide hypothesis. Susceptibilities of uranium solutions were first reported by Lawrence,<sup>17</sup> and a few magnetic studies extending to the light actinides in solution were first performed under the auspices of the Manhattan District Project and published in the postwar period.<sup>18–20</sup> A more extensive investigation was reported by Howland and Calvin.<sup>21</sup> A study

Received: September 18, 2013

Published: February 7, 2014

**Table 1. Cations Studied Showing Their Nominal f Orbital Configuration, the Resulting Number of Unpaired Electrons, the Specific Media Conditions: Perchloric Acid and Actinide Concentrations Employed**

cation	f orbital configuration	number of unpaired electrons	[HClO <sub>4</sub> ] mol L <sup>-1</sup>	[An <sup>n+</sup> ] 10 <sup>-3</sup> mol L <sup>-1</sup>
Th(IV)	f <sup>0</sup>	0	1	210 ± 7 and 145 ± 5
U(IV)	f <sup>2</sup>	2	0.1	15.1 ± 0.4
U(IV)	f <sup>2</sup>	2	1	42.0 ± 1
U(VI)	f <sup>0</sup>	0	1	207 ± 4 and 530 ± 1
Np(IV)	f <sup>3</sup>	3	1.1	45.0 ± 0.8
Np(IV)	f <sup>3</sup>	3	1	37.0 ± 0.6
Np(V)	f <sup>2</sup>	2	1	41.7 ± 1.7
Np(VI)	f <sup>1</sup>	1	1	31.2 ± 0.9
Pu(III)	f <sup>5</sup>	5	2	138 ± 6
Pu(IV)	f <sup>4</sup>	4	2	43.9 ± 1.8
Pu(IV)	f <sup>4</sup>	4	1	21.4 ± 0.6
Pu(VI)	f <sup>2</sup>	2	2	31 ± 0.9 and 49 ± 0.5
Pu(VI)	f <sup>2</sup>	2	1	19.8 ± 0.2
Am(III)	f <sup>6</sup>	6	1	96.0 ± 2
Cm(III)	f <sup>7</sup>	7	1	0.668 ± 0.01 and 2.17 ± 0.03
Cf(III)	f <sup>9</sup>	5	1	0.738 ± 0.03

by Lewis and Calvin employed a bifilar suspension method, inspired from one described by Theorell,<sup>23</sup> for making magnetic susceptibility measurements in solution.<sup>22</sup> Dispersed hydrochloric, sulfuric, or nitric acid solutions of uranium through americium were studied using this technique.

The systematic determination of actinide paramagnetic behavior provides information about the number of unpaired electrons and their electronic states. To compare actinide to lanthanide bare hydrated ions, the study has been undertaken in perchloric media. Under these conditions the first coordination sphere is typically composed of solvating water molecules, avoiding as much as possible numerous species that could be formed in more chelating media like nitrate or chloride. Furthermore, water molecules are considered to be a weak ligand from a spectrochemical series perspective.

In this Work, we report magnetic susceptibility measurements for all of the actinide cations with sufficient stability to be of importance and commonly encountered in radiochemical laboratory and reprocessing work. Magnetic susceptibility was measured in each case in perchloric acid, by use of NMR with Evans method.<sup>24–31</sup> We have previously demonstrated this technique using americium,<sup>32</sup> and Braekers has reported using this method with neptunium.<sup>33</sup> To our knowledge, this is the first comprehensive examination of actinide ion susceptibility using NMR. This work will serve as a foundation for extending the many valuable modern NMR techniques to the actinide elements.

## EXPERIMENTAL SECTION

**Preparation of the NMR Samples.** All actinide stocks were drawn from existing solutions or solids prepared at CEA Marcoule, except as noted. The solution acidities were adjusted using stock solutions of perchloric acid prepared from concentrated perchloric acid. For all the cations examined, oxidation states were checked by UV–visible (UV–vis) spectrophotometry just prior to and immediately after each NMR experiment (Figures S1–S6 in Supporting Information). The concentrations of the solutions were determined by UV–vis spectrophotometry and  $\alpha$  and/or  $\gamma$  spectroscopies as appropriate (see Table 1).

**Caution!** All of the actinide elements are radioactive and should be handled only in facilities that are specially equipped and approved for radioactive work. In particular, Pu-239, Am-241, Cm-244, and Cf-249 are high specific activity radionuclides.

The U(IV) solution was prepared under inert atmosphere by dissolving solid UCl<sub>4</sub> (M = 380 g/mol), supplied by IPN Orsay, in 0.1 and 1 M perchloric acid and adding silver perchlorate to precipitate the chloride present.

Stock solutions of Np(V) were prepared by dissolving a known mass of NpO<sub>2</sub>OH·2.5H<sub>2</sub>O (M = 331 g/mol) in 1 M perchloric acid. Hexavalent neptunyl was prepared by oxidizing a Np(V) solution to obtain a 1 M perchloric acid with an excess (ca. 4 equiv) of silver oxide. The silver(I) ions were removed by precipitation, using addition of 1 M hydrochloric acid. Tetravalent neptunium was prepared by reducing a Np(V) solution with hydroxylammonium perchlorate (6 M) in 1 M perchloric acid at 80 °C. The conversion of neptunium from Np(V) to Np(IV) was demonstrated spectrophotometrically to be greater than 99% efficient.

The isotopic composition of the plutonium stock used for the Pu(III) studies was 0.081% 238, 80.592% 239, 17.145% 240, 1.810% 241, and 0.372% 242. The Pu(IV) and Pu(VI) studies were performed using a different stock solution with a composition of 0.017% 238, 96.91% 239, 2.99% 240, 0.065% 241, and 0.009% 242. The Pu(III) was prepared by dissolving Pu(OH)<sub>4</sub> (s) precipitate in an appropriate volume of perchloric acid and then treating the solution with solid hydroxylamine hydrochloride. The chloride introduced by the hydroxylamine salt was removed by precipitation, using a stoichiometric amount of silver perchlorate. A stock solution of Pu(VI) in 2 M perchloric acid was prepared from thermal decomposition (to white fumes) of an existing plutonium perchlorate solution and was used to prepare Pu(VI) and Pu(IV) samples. The Pu(VI) solution was prepared by diluting a known volume of the Pu(VI) stock solution in 2 M perchloric acid. The Pu(IV) solution was prepared by reducing a known volume of Pu(VI) stock solution with hydroxylammonium perchlorate in 2 M perchloric acid. The conversion of plutonium from Pu(VI) to Pu(IV) was demonstrated spectrophotometrically to be greater than 99% efficient.

The americium was prepared from a stock solution of Am(III) nitrate. The isotopic composition of the stock americium was 98.74% 241, <0.02% 242, and 1.25% 243. Americium hydroxide was initially formed by adding aliquots of sodium hydroxide to the solution. The sample was subsequently prepared by dissolving this solid in an appropriate volume of perchloric acid to obtain the desired working solutions. The concentration of americium was checked by UV–vis and  $\gamma$  spectrometries. Trace impurities of Fe(III) (<0.3 atom percent (%)) and Nd(III) (<0.02 atom %) were detected by inductively coupled plasma spectrometer (ICP) coupled to a sector field mass spectrometer in the Am(III) perchlorate solution (96.0 mM). Radiotracer quantities of Cm were also detected in the Am solution (1.4 × 10<sup>8</sup> Bq/L of Cm-242 and 1.1 × 10<sup>9</sup> Bq/L of Cm-243 + Cm-244).

The curium-244 solution was recovered from an ill-defined organic compound by sequentially heating it to dryness in concentrated nitric acid and then perchloric acid. The residue was redissolved in nitric acid and purified on a dedicated Eichrom LN resin column. The eluted fraction was concentrated to dryness and redissolved in perchloric acid. The concentration of curium and the absence of Pu-240 daughter product was checked by  $\alpha$  spectroscopy.

The californium-249 sample used was a perchlorate solution prepared at IPN Orsay for a previous study. The solution was purified through a series of ion exchange columns and fuming to dryness.<sup>34</sup> Earlier studies using this same californium sample trace the origins of this stock back to its production.<sup>35</sup> The californium(III) solution was examined by  $\gamma$  and UV-vis spectroscopies to verify concentration and purity.

**Evans NMR Method.** For the NMR experiments, a Varian Inova 400 MHz spectrometer running Varian NMR 6.3.c was used for all of the studies. The samples were referenced against an external *tert*-butanol signal following the Evans method.<sup>24–31</sup> Specific challenges and treatment of the data are discussed later as they relate to temperature. The external reference was prepared at the same acid concentration but in deuterated water to provide a lock signal. The samples were prepared at the acidities noted in Table 1. All of the samples were doubly contained by loading the sample into a 3.0 mm i.d. polytetrafluoroethylene (PTFE) inner tube (liner) with the reference solution in the outer glass 5.0 mm NMR tube, as illustrated in Figure 1. For the microscale amounts of solution employed in the

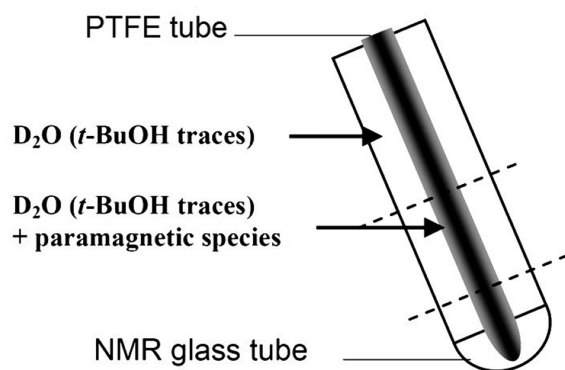


**Figure 1.** Experimental setup for all measurements.

Cf studies, the working solution was loaded into a 1.0 mm X-ray diffraction (XRD) capillary tube fitted in the PTFE liner. Experiments with the Cm(III) sample were carried out, both with a liner and using a 1.5 mm XRD capillary, to check whether the use of the insert caused any difference in sample properties. Bulk magnetic susceptibility (BMS) in both cases agreed, with a deviation of less than 1%.

Variable-temperature studies were performed to verify that a Curie-like behavior ( $\chi^{-1}$  linear with  $T$ ) was present under the conditions used for the calculations. In general, the paramagnetically induced shifts were checked every 5 °C from 5 to 50 °C. For all comparative discussions in this Work, the data at 25 °C were used.

## RESULTS AND DISCUSSION

**General Considerations about Lanthanide and Actinide Magnetism.** Any species that has one or more unpaired electron is paramagnetic and thus possesses a magnetic moment  $\mu$ . Assuming a Boltzmann distribution of individual magnetic dipoles  $\mu$  along an external magnetic field  $\vec{B}$ , the resulting magnetization  $\vec{M}$  of a solution containing paramagnetic cations follows the Langevin equation. Except for very low temperatures (around those of liquid helium), in moderate magnetic fields (less than a few tenths of a T) the ratio  $\mu\vec{B}/k_{\text{B}}T \ll 1$  ( $k_{\text{B}}$  being the Boltzmann constant). Then an approximation

of Langevin's equation can be applied, giving rise to the Curie law:

$$\vec{M} = \frac{N_A \mu^2 \vec{B}}{3k_{\text{B}}T} \quad (1)$$

From magnetic susceptibility definition:  $\chi = \partial\vec{M}/\partial\vec{H}$  and  $\vec{B} = \mu_0(\vec{H} + \vec{M})$ , assuming  $\chi \ll 1$ , which is the case in our study,  $\mu_0 = 4\pi \times 10^{-7}$ , the magnetic susceptibility can be written as

$$\chi = \mu_0 \frac{\vec{M}}{\vec{B}} \quad (2)$$

and from eq 1 it can be shown that

$$\chi = \mu_0 \frac{N_A \mu_{\text{B}}^2 \mu_{\text{eff}}^2}{3k_{\text{B}}T} \equiv \frac{C}{T} \quad (3)$$

where  $\mu_{\text{eff}}$  is the magnetic moment in Bohr magneton unit  $\mu_{\text{B}}$  and  $C$  is the Curie constant. A quantum description taking into account a spin system with two levels would lead to the same result through the Brillouin function.

Thus, for most paramagnetic compounds, the magnetic susceptibility  $\chi$  is inversely proportional to the absolute temperature  $T$ . However, in the case of a second magnetic field  $\vec{B}_{\text{mol}}$  arising from electrons or atoms in the vicinity of the paramagnetic cation, the resulting field is  $\vec{B} + \vec{B}_{\text{mol}}$ . From Weiss' assumption, suggesting this extra field is proportional and collinear to the resulting magnetization ( $\vec{B}_{\text{mol}} = \lambda\vec{M}$ ), it is seen that

$$M = \frac{B}{\mu_0} \frac{C}{T - \theta} \quad (4)$$

with  $C$  and  $\theta$  being the Curie and Weiss constants, respectively. The magnetic susceptibility is then

$$\chi = \frac{C}{T - \theta} \quad (5)$$

In practice this law is only relevant for temperatures greater than the Curie temperature ( $T > \theta$ ) and is mainly observed to apply to solid-state compounds. Magnetic susceptibility follows a Curie law but rapidly increases to infinity when  $T$  approaches the  $\theta$  value. From the sign of  $\theta$ , ferro-, ferri- or antiferromagnetic interactions can be deduced, revealing the relative arrangement of the magnetic moments. In regard to actinides, Nave et al.<sup>16</sup> experimentally determined effective magnetic moments and Curie–Weiss constants for some  $f^6$  and  $f^7$  actinide compounds in the temperature range from 4 to 300 K, while in our Study the temperature span is much narrower (mainly from 278 K (5 °C) to 323 K (50 °C)).

Deviation from the Curie law may also occur in diluted compounds and in a narrow temperature range (0 to 50 K) but for other reasons: Hendricks et al.,<sup>36</sup> who measured magnetic susceptibility of Cm<sup>3+</sup> diluted in a Cs<sub>2</sub>NaLuCl<sub>6</sub> diamagnetic compound, attributed the Curie-law deviation to crystal-field splitting of Cm<sup>3+</sup> and determined a Curie–Weiss temperature. Crystal- or ligand-field effect is then of primary importance.

A more comprehensive description of paramagnetic behavior may be given especially when several energy states are involved for a given spin system. That is the case of Eu(III)<sup>37</sup> and Sm(III), for which the Van Vleck equation<sup>38</sup> has to be applied to get magnetic susceptibility versus temperature:

**Table 2.** Experimental Molar Magnetic Susceptibility  $\chi_M$  and Effective Magnetic Moments  $\mu_{\text{eff}}$  Calculated from Equations 11 and 12

ox. state	actinide	f orbital conf.	ground state	Hund's rule		experimental values	
				$\chi_M$ ( $10^{-9}$ m <sup>3</sup> /mol)	$\mu_{\text{eff}}$ ( $\mu_B$ )	$\chi_M$ ( $10^{-9}$ m <sup>3</sup> /mol)	$\mu_{\text{eff}}$ ( $\mu_B$ )
III	Pu	f <sup>5</sup>	<sup>6</sup> H <sub>5/2</sub>	3.78	0.85	7.8 ( $\pm 0.2$ )	1.22 ( $\pm 0.02$ )
	Am	f <sup>6</sup>	<sup>7</sup> F <sub>0</sub>		0	14.1 ( $\pm 0.2$ )	1.64 ( $\pm 0.01$ )
	Cm	f <sup>7</sup>	<sup>8</sup> S <sub>7/2</sub>	333	7.94	354 ( $\pm 7$ )	8.20 ( $\pm 0.08$ )
	Cf	f <sup>9</sup>	<sup>6</sup> H <sub>15/2</sub>	599	10.65	736 ( $\pm 31$ )	11.8 ( $\pm 0.2$ )
IV	Th	f <sup>0</sup>	<sup>1</sup> S <sub>0</sub>	0	0	-0.68 ( $\pm 0.05$ )	0 <sup>a</sup>
	U	f <sup>2</sup>	<sup>3</sup> H <sub>4</sub>	67.7	3.58	53.7 ( $\pm 2$ )	3.19 ( $\pm 0.06$ )
	Np	f <sup>3</sup>	<sup>4</sup> I <sub>9/2</sub>	69.2	3.62	46.4 ( $\pm 2$ )	2.97 ( $\pm 0.06$ )
	Pu	f <sup>4</sup>	<sup>5</sup> I <sub>4</sub>	38.1	2.68	28.1 ( $\pm 0.2$ )	2.31 ( $\pm 0.01$ )
V	Np	f <sup>2</sup>	<sup>3</sup> H <sub>4</sub>	67.7	3.58	49.2 ( $\pm 1$ )	3.06 ( $\pm 0.03$ )
VI	U	f <sup>0</sup>	<sup>1</sup> S <sub>0</sub>	0	0	0.78 ( $\pm 0.03$ ) <sup>b</sup>	0.385 ( $\pm 0.002$ )
	Np	f <sup>1</sup>	<sup>2</sup> F <sub>5/2</sub>	34.0	2.54	27.6 ( $\pm 0.5$ )	2.29 ( $\pm 0.02$ )
	Pu	f <sup>2</sup>	<sup>3</sup> H <sub>4</sub>	67.7	3.58	71.4 ( $\pm 3$ )	3.68 ( $\pm 0.08$ )

<sup>a</sup>At 25 °C for all studied actinide cations. <sup>b</sup>In the U(VI) case, the  $\chi_M$  value applies at any temperature because of its TIP. Magnetic susceptibility and effective magnetic moment corresponding to the ground states are calculated according to eqs 9 and 7, respectively. All values are in SI units.

$$\chi = \frac{N_A \sum_i \left[ \frac{(E_i^{(1)})^2}{k_B T} - 2E_i^{(2)} \right] \exp \left[ -E_i^{(0)}/k_B T \right]}{\sum_i \exp \left[ -E_i^{(0)}/k_B T \right]} \quad (6)$$

where  $E_i^{(0)}$  is the energy of the level  $i$ , with no magnetic field.  $E_i^{(1)}$  and  $E_i^{(2)}$  are, respectively, Zeeman energy first and second order of level  $i$ . When only one level (the ground state) is involved,  $E^{(0)}$  is set to 0, and  $\chi$  follows a Curie-law relationship if there is no second-order Zeeman energy involved. That is mainly the case encountered for paramagnetic lanthanide (III) ions, assuming the energy levels are simply arising from first-order Zeeman splitting of an isolated state of a free ion  $E^{(1)} = g\mathbf{H}\mu_B\mu_{\text{eff}}$ .

The magnetic moment can be readily calculated at room temperature using Hund's rule,<sup>39</sup> which states the quantum numbers ( $L$ ,  $S$ , and  $J$ , which represent, respectively, orbital, quantum spin, and total angular momentum numbers) of the more stable electronic state. Thus, the effective magnetic moment is expressed as

$$\mu_{\text{eff}} = g\sqrt{J(J+1)} \quad (7)$$

where the Landé factor  $g$  is defined as

$$g = 1 + \frac{J(J+1) + S(S+1) - L(L+1)}{2J(J+1)} \quad (8)$$

and it follows that

$$\chi = \mu_0 \frac{N_A g^2 \mu_B^2 J(J+1)}{3k_B T} \quad (9)$$

which is eq 3. At room temperature, Hund's prediction agreed well with experimental magnetic moments, except for samarium(III) and europium(III), as mentioned above.

In regard to actinide (III) ions, recent work by Apostolidis reported  $[\text{An}(\text{H}_2\text{O})_9](\text{CF}_3\text{SO}_3)_3$  magnetic susceptibility measurements in the solid state ( $\text{An} = \text{U}$  to  $\text{Am}$ ).<sup>40</sup> Ligand-field calculations with nine water molecules in a  $C_{3h}$  symmetry was used to explain experimental data. A good agreement was observed for U(III), but discrepancies observed for Np(III) and Am(III) at low temperature (below 100 K) were attributed to paramagnetic impurities. A slight deviation around 300 K is

observed for Pu(III), but the authors stated that the overall behavior along the series is consistent with that expected for noninteracting  $\text{An}^{3+}$  ions. In the U(III) case, their density functional theory (DFT) calculations, taking into account the ground-state <sup>4</sup>I<sub>9/2</sub> degeneracy splitting due to the crystal field, reproduced the experimental magnetic susceptibility over a large temperature range especially below 100 K, where a deviation from the Curie law is observed. Similarly, deviation from Curie law was observed for samarium(III) sulfate octahydrate at low temperature (below 160 K). Van Vleck, in 1947, reported that, at such temperature, the cation is no longer isolated from surrounding ions, and thus the cubic crystal-field effect must be considered.<sup>41</sup> The ligand field splits the  $J = 5/2$  ground-state level into two levels with a 207 cm<sup>-1</sup> gap, which is sufficient to explain the experimental decay of the effective magnetic moment values.

Nevertheless, one can see that over a short temperature range (~100K) around room temperature, magnetic susceptibility curves reasonably follow a  $1/T$  relationship. This is an important point in the framework of our study (which deals with temperatures from 278 to 323 K) to demonstrate the validity of eq 9 because it readily allows the calculation of magnetic moments from experimental magnetic susceptibility measurements.

**Experimental Measurements.** In the Evans method,<sup>24–30</sup> the shift observed between the reference and the working solution of *tert*-butanol signals ( $\Delta\delta = \delta_{\text{alcohol+actinide}} - \delta_{\text{alcohol}}$ ) is directly related to the difference of molar magnetic susceptibility  $\chi_M$  as follow:

$$\chi_M = \frac{3\Delta\delta}{10^3[\text{An}^{n+}]} \quad (10)$$

where  $\Delta\delta$  is dimensionless because it is a relative frequency shift ( $\Delta\nu/\nu_0$  with  $\nu_0 = 399.948 \times 10^6$  Hz the operating NMR frequency) and a positive value for paramagnetic behavior,  $[\text{An}^{n+}]$  the molar concentration (mol/L) of the paramagnetic element, and  $\chi_M$  the sample molar magnetic susceptibility (m<sup>3</sup>/mol) in the International System (SI) of units. The solvent magnetic susceptibility has been neglected, as suggested by Grant,<sup>28</sup> for small paramagnetic molecules. However because we used deuterated water only in the reference solution, we have checked whether a solvent magnetic susceptibility could

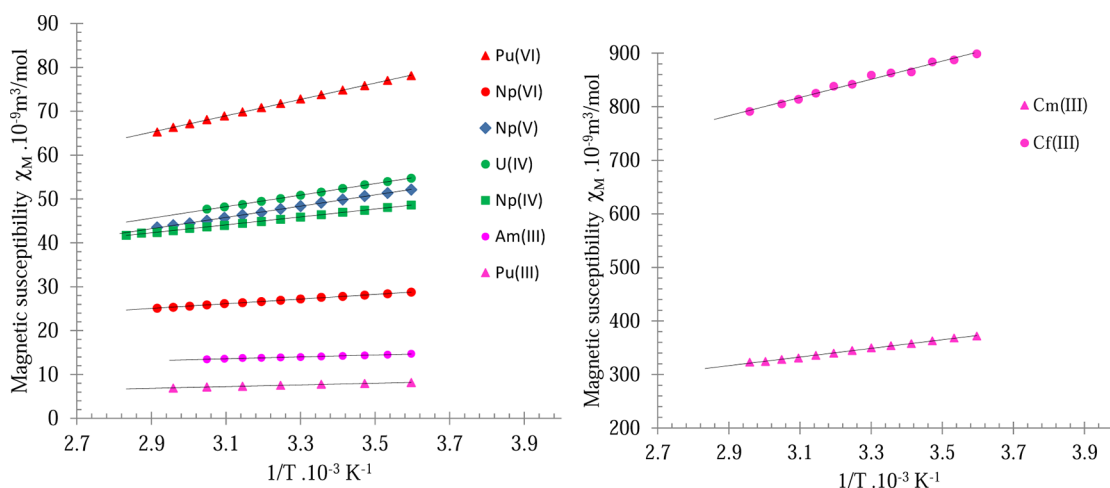


**Figure 2.** Experimental magnetic susceptibility of actinide cations in perchloric media vs  $1/T$  from 5 to 80 °C.

have an effect on the actinide BMS measurements. It appeared that molar susceptibilities we measured  $\chi_{\text{H}_2\text{O}}^{20^\circ\text{C}} = -1.63 \times 10^{-10} \text{ m}^3/\text{mol}$  and  $\chi_{\text{D}_2\text{O}}^{20^\circ\text{C}} = -1.60 \times 10^{-10} \text{ m}^3/\text{mol}$  are quite similar, and no specific “solvent correction” is required in eq 10.

The measured magnetic susceptibility  $\chi_M$  is defined as the sum of diamagnetic  $\chi_D$  and paramagnetic  $\chi_P$  contributions. Actinide ions having unpaired electrons also have abundant other paired electrons and may display diamagnetism. To get paramagnetic effects only arising from actinide ions, diamagnetic corrections should be applied to BMS measurements:  $\chi_P = \chi_M - \chi_D$ . Diamagnetic corrections can be calculated either from Pascal’s constants, using either Angus’s or Slater’s methods, or they can be deduced from our Th(IV) BMS measurements. The first way, based on an additive fashion using values for the diamagnetic susceptibility of every atom,<sup>42</sup> leads to  $-0.29 \times 10^{-9}$  and  $-0.39 \times 10^{-9} \text{ m}^3/\text{mol}$  for Th(IV) and U(VI), respectively (calculation in U(VI) case depends on  $\text{O}^{2-}$  constant sources). No value is available for Am(III) or Pu(III) cations, but a  $-0.58 \times 10^{-9} \text{ m}^3/\text{mol}$  value is tabulated for U(III). Angus’s method applied to  $\text{Th}^{4+}$  ion gives  $\chi_D = -0.39 \times 10^{-9} \text{ m}^3/\text{mol}$  and  $-0.42 \times 10^{-9} \text{ m}^3/\text{mol}$  for  $\text{Pu}^{3+}$  and  $\text{Am}^{3+}$  ions. The precision of the cation diamagnetism measurements is not very good, but these values give an idea of the magnitude of the diamagnetic effects that we can expect. They will be discussed when required, that is, for Th(IV), Pu(III), Am(III), and U(VI). In all other cases, diamagnetic corrections are weaker than the experimental accuracy we determined. For this reason, all experimental magnetic susceptibilities are tabulated in Table 2 without any diamagnetic correction.

BMS errors are computed from eq 10, taking into account the error in the cation concentration from  $\alpha$  or  $\gamma$  spectrometry and/or UV–vis spectrophotometry. In the Th(IV) and U(VI) cases, the X-ray fluorescence spectrometer was used to determine cation concentrations. Errors in NMR chemical shift measurements depend on spectra digital resolution that is about 0.001 ppm. They can therefore be neglected compared to concentration errors, except for small BMS values, for which chemical shift variations are the same order of magnitude as the resolution. In such a situation, the NMR error is estimated from chemical shift variations versus  $1/T$ . In the Th(IV) case, NMR measurement errors could be as large as 7%, despite the high cation concentration used. When different experimental

conditions were employed for one actinide ion (see Table 1), the average BMS and the corresponding deviation is reported in Table 2.

Assuming cations follow a Curie law in the temperature range, eq 3 can be combine with eq 10, and the observed shift  $\Delta\delta$  can be directly related to the effective magnetic moment  $\mu_{\text{eff}}$  of the working solution paramagnetic cation as follows:

$$\mu_{\text{eff}} = 798 \sqrt{\frac{3\Delta\delta}{10^3[\text{An}^{n+}]}} T = 798 \sqrt{\chi_M T} \quad (11)$$

Values from eqs 10 and 11 can be expressed in emu–cgs units by dividing them by a conversion factor of  $4\pi \times 10^{-6}$ .

In the case of diamagnetic behavior ( $\chi_M < 0$ ), the effective magnetic moment  $\mu_{\text{eff}}$  can be calculated from eq 2 and considering the magnetization of the sample  $M = N\mu = N\mu_{\text{eff}}\mu_B$ , with  $N$  the number of atoms per unit volume ( $N = 10^3 N_A [\text{An}^{n+}]$ ). The effective magnetic moment is therefore:

$$\mu_{\text{eff}} = \frac{\chi \mathbf{B}_0}{10^3 \mu_0 \mu_B N_A [\text{An}^{n+}]} \quad (12)$$

where  $\mathbf{B}_0 = 9.4 \text{ T}$  (the magnet field magnitude of our NMR spectrometer),  $N_A = \text{Avogadro's number}$ , the Bohr magneton  $\mu_B = 9.27 \times 10^{-24} \text{ J T}^{-1}$ , and  $[\text{An}^{n+}] = \text{actinide concentration in mol L}^{-1}$ .

## EXPERIMENTAL RESULTS

### Temperature Dependence of the Magnetic Susceptibilities.

Molar magnetic susceptibilities  $\chi_M$  were calculated in SI units from variation of *tert*-butanol chemical shifts ( $\Delta\delta$  values) at different temperatures, using eq 10. The temperature range examined was from 5 to 55 °C at minimum (Am(III) study) and up to 85 °C in the Pu(IV) case. Because of increased temperatures and probably radiolytic effects, bubbles formed, creating field inhomogeneities that distorted NMR signals in some of the studies at higher temperatures. In most cases, this problem was overcome by removing the NMR tubes assembly from the magnet and returning them to the glovebox for some gentle agitation. However, with the  $^{241}\text{Am(III)}$  samples, bubbles appeared faster than the required time to reach higher equilibrium temperatures in the magnet.

Despite the short temperature range available for the perchlorate work, most of the samples follow a Curie or at least a Curie-like law. Results plotted in Figure 2 as  $\chi_M$  versus  $1/T$  exhibit good linear correlation coefficients ( $r^2 > 0.992$ ), indicating that the relative occupancy of the electronic states does not change significantly over the temperature range studied. As can be seen from the plots, there is a

nearly 1 order of magnitude difference between less than and more than half-filled 5f orbitals. For all cations except Th(IV) effective magnetic moments were calculated according to eq 11, as reported in Table 2.

The Th(IV) and U(VI) BMS temperature dependencies are shown in Figure 3 as a function of  $1/T$  and compared to HClO<sub>4</sub> magnetic

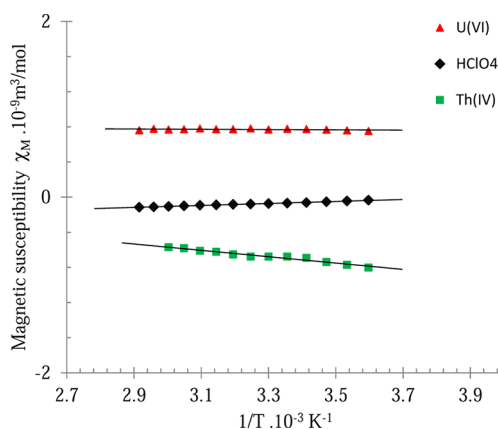


**Figure 3.** Experimental magnetic susceptibilities of Th(IV) and U(VI) in 1 M perchloric media vs  $1/T$  from 5 to 80 °C. Black squares are molar magnetic susceptibilities of a 1 M perchloric acid blank collected at different temperatures.

susceptibility behavior. The U(VI) slope is negative like those of Th(IV) but twenty times smaller. The low correlation coefficient value obtained (below 0.42) indicates U(VI) BMS does not significantly change in the studied temperature range. Taking into account a diamagnetic contribution of  $-0.39 \times 10^{-9} \text{ m}^3/\text{mol}$  from Pascal's constants, a small but positive U(VI) BMS value ( $\chi = 0.24 \times 10^{-9} \text{ m}^3/\text{mol}$ ) indicates a paramagnetic behavior, which has already been explored.<sup>43</sup> This can be explained thanks to the second order Zeeman effect in the Van Vleck equation (eq 6) since the ground state ( $^1S_0$ ) as defined by Hund's rule would lead to a nonmagnetic behavior. This description is completely in agreement with the temperature-independent paramagnetic (TIP) behavior of U(VI) we observed, considering our experimental accuracy.

As expected, a negative BMS value indicates a diamagnetic behavior for the Th(IV) cation, but a negative slope is observed instead of a relatively flat dependence as seen the U(VI) case. This slight temperature dependence has previously been reported in the literature but is still not understood.<sup>44</sup> Diamagnetic susceptibilities tabulated from Pascal's constants or calculated from Angus's method are both the same order of magnitude as our experimental value, differing by a factor of 2. Considering the diamagnetic contribution arising from nine water molecules surrounding the Th(IV) cation, the  $[\text{Th}(\text{H}_2\text{O})_9]^{4+}$  diamagnetic susceptibility calculated from Pascal's constants<sup>42</sup> leads to  $-1.76 \times 10^{-9} \text{ m}^3/\text{mol}$ , which is roughly twice our experimental value.

The magnetic susceptibility of Am(III) was observed to be 1 order of magnitude larger than that of U(VI) and twice that of Pu(III), with a  $1/T$  dependence similar to that of Pu(III). These measurements are surprising because the theoretical descriptions predict a state  $J = 0$ , a nonmagnetic state, and second, the first excited state is about 2700  $\text{cm}^{-1}$  above the ground state. On the other hand, Soderholm et al. found a low and temperature-independent paramagnetism (TIP) behavior that they explained was due to a large second-order Zeeman effect arising from  $J$  mixing contributions with a higher energy state.<sup>45</sup> Experimental difficulties evoked earlier could account for the Curie-like law dependence of Am(III) that we observed, but among the Am(III) experiments we carried out (only one is mentioned in Table 1), we noticed that Am(III) BMS were slightly concentration-dependent.

Considering Pu(IV) magnetic susceptibility versus  $1/T$ , a clear break appears around 40 °C, revealing a nearly constant (slightly increasing) magnetic susceptibility as temperature increases (Figure 4).

Pu(IV) and Np(VI) have similar BMS magnitudes but clearly exhibit different temperature behavior in perchloric media.

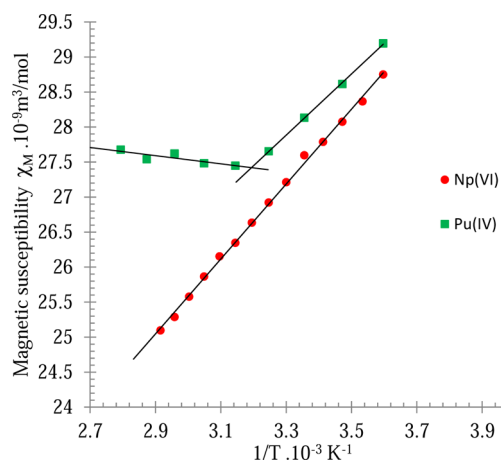
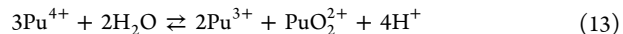


**Figure 4.** Comparison of Pu(IV) and Np(VI) experimental magnetic susceptibilities in perchloric media vs  $1/T$  from 5 to 80 °C.

From experimental conditions, we can see that UV-vis spectra (Figure S3 in Supporting Information) prove that a slight amount of Pu(VI) polluted the Pu(IV) working solution. The large Pu(VI) molar extinction coefficient and the observed weak absorbance from Pu(VI) suggests only trace amount of Pu(VI), such that the magnetic susceptibility effect could be neglected, especially since no significant optical density change was observed before and after NMR experiments. However, we noticed differences in Pu(IV) BMS measurements comparing 1 and 2 mol L<sup>-1</sup> perchloric media. In the former case the curve break appeared 5 °C sooner, with the BMS clearly increasing as  $T$  increases. Other Pu(IV) BMS measurements, performed at 50 °C for several hours with UV-vis spectra recorded simultaneously, confirmed that the BMS increase is correlated to an increase in the concentration of Pu(VI). This Pu(VI) formation, explained<sup>46</sup> by the disproportionation of Pu(IV), is extremely weak during the Pu(IV) BMS measurements (about  $10^{-4} \text{ mol L}^{-1}$ ). Taking into account species from the equilibrium eq 13, we can see that Pu(IV) contamination is offset by Pu(VI) with a magnetic susceptibility that is 3 times greater than that of Pu(IV). However, Pu(III) ingrowth also contributes to the curve break observed for Pu(IV) BMS, despite its low BMS value, about 4 times smaller than that of Pu(IV).



**Magnetic Susceptibilities at Room Temperature.** The experimentally determined molar magnetic susceptibility  $\chi_M$  values and their corresponding effective magnetic moments  $\mu_{\text{eff}}$  at 25 °C are summarized Table 2 and compared to the theoretical susceptibility and magnetic moments of the free ions, derived by assuming that the ground state is defined by Hund's rule and L-S coupling. Calculations depend on the validity of eqs 7 and 9 and assume that excited states are far enough from the ground state to be thermally populated.

As shown Figure 5, the experimental magnetic susceptibilities roughly follow the predicted shape from Hund's rule (dashed line) and are in agreement with Howland and Calvin<sup>21</sup> data even though those samples were prepared in various (hydrochloric, sulfuric, and nitric) weakly acidic aqueous phases. However, considering the isoelectronic configuration, there are significant deviations depending on the oxidation state: An(IV) but more importantly An(V) has experimental values lower than those calculated from eq 7. Conversely, some actinide(III) ions such as Am(III) and Cf(III) have experimental magnetic susceptibilities higher than those predicted from Hund's rule. Furthermore, despite Pu(III) and Am(III) having similar oxidation state and f electronic configuration compared to Sm(III) and Eu(III), one can see from Figure 5 they behave differently. We will discuss these results with values from literature.

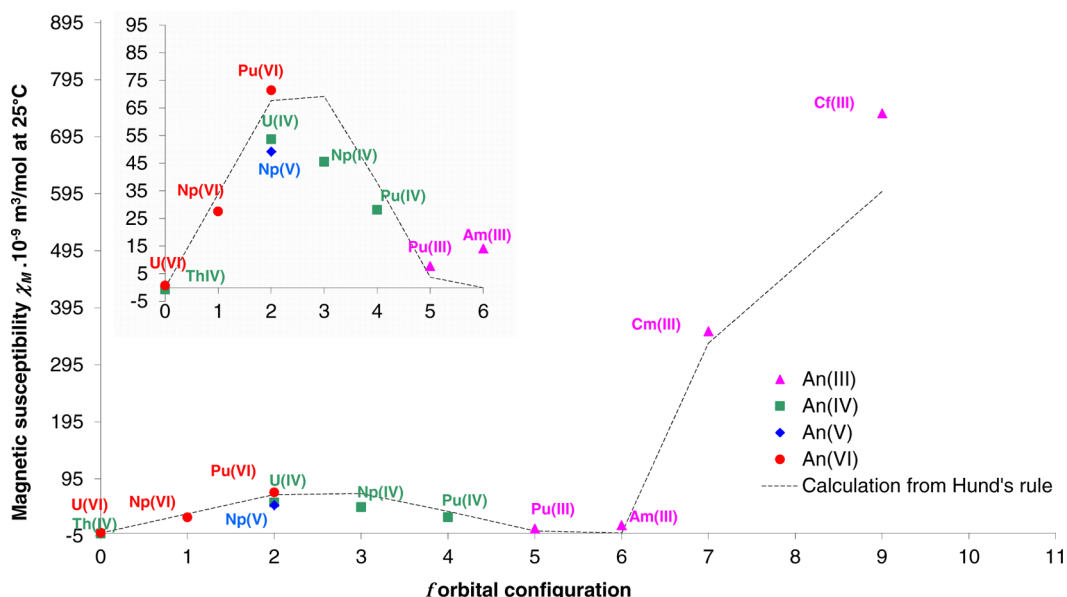


**Figure 5.** Magnetic susceptibilities of actinide cations studied as a function of their electronic configuration at 25 °C. Dashed lines are theoretical calculations according to eqs 9

**Oxidation State Three.** Considering the trivalent actinides as the set of cations more directly comparable to the trivalent lanthanides, it is noteworthy that a deviation from the Hund's rule calculations is present in Table 2 and in the dashed line in Figure 5. The only instances of such deviations in the lanthanide series are seen for Sm(III) ( $4f^5$ ) and Eu(III) ( $4f^6$ ) ions, where a deviation of effective magnetic moment from Hund's rule (plain line in Supporting Information, Figure S7) is expected and explained by taking into account partial occupancy of low-lying excited states in the Van Vleck calculations. Considering the actinides with isoelectronic configuration to Sm(III) and Eu(III), namely Pu(III) and Am(III), it is noted that both fall short of the plain curves in Supporting Information, Figure S7. This exhibits clearly that 5f orbitals behave differently from the homologous 4f orbitals. From optical properties of actinide(III) ions<sup>47</sup> it is clear that the first excited states are several thousand  $\text{cm}^{-1}$  above the ground state and thus cannot be used to explain the discrepancies in magnetic susceptibility.

In recent DFT calculations, Apostolidis et al.<sup>40</sup> confirmed the first  $\text{Am}^{3+}$  magnetic state belonging to the  $^3F_1$  multiplet approximately 1740  $\text{cm}^{-1}$  above the ground state  $^7F_0$  is too high in energy to be populated. Their experimental magnetic susceptibility curve versus temperature above 30 K of a  $[\text{Am}(\text{H}_2\text{O})_9](\text{CF}_3\text{SO}_3)_3$  crystal was found to be constant and reasonably consistent with a nonmagnetic behavior ( $J = 0$ ). Though not reporting precise susceptibility values for Am(III), they found  $\text{Am}^{3+}$  BMS smaller than that of Pu(III). This result is in contrast with our BMS measurements in perchloric solution, wherein the Am(III) BMS appears to be twice that of Pu(III) at 25 °C. Our BMS Am(III) value is double that of the magnetic susceptibilities reported from SQUID magnetometers measurements with  $\text{AmF}_3$  ( $8.97 \times 10^{-9} \text{ m}^3/\text{mol}$ )<sup>45</sup> and  $\text{Cs}_2\text{NaAmCl}_6$  ( $8.17 \times 10^{-9} \text{ m}^3/\text{mol}$ )<sup>16</sup> compounds. Paramagnetic impurities can account for odd experimental magnetic susceptibility, particularly for an actinide with expected low values such as Am(III).<sup>45</sup> However, as noted briefly in the Experimental section, the mass spectroscopy, showing iron and curium trace contaminations in the Am stock, reveals that the amounts involved are insufficient to significantly affect the magnetic susceptibility measurements. On the other hand this Work employed mainly the Am-241 isotope(III), while most other authors used the lower specific activity Am-243 isotope. The higher specific activity of the Am-241 isotope may have significantly impacted the formation of radical species generated by water radiolysis and led to increasing BMS measurements. Similarly, Pu(III) BMS reported by Apostolidis et al.<sup>40</sup> (about  $3.43 \times 10^{-9} \text{ m}^3/\text{mol}$  for a  $[\text{Pu}(\text{H}_2\text{O})_9](\text{CF}_3\text{SO}_3)_3$  solid

compound at 25 °C) is twice lower than the value we measured in perchloric solution by using a long half-life Pu-242 isotope, while ours is mainly Pu-239. Diamagnetic corrections are negligible on Pu(III) (as they are for Am(III) as well). Specific activities are 0.1 GBq/g and  $17.6 \times 10^3 \text{ GBq/g}$ , respectively. So radiolysis effects are not a clear explanation of Am(III) discrepancies with literature.

Regarding Cm(III) the effective magnetic moment in perchloric solution (Table 2, Supporting Information, Figure S7) appears slightly higher than published values ( $7.9 \mu_B$ ,<sup>36</sup>  $7.89 \mu_B$ ,<sup>48</sup>  $7.74 \mu_B$ <sup>16</sup>). This difference is unlikely to be due to experimental errors since the Evans method was performed twice (once in a capillary and once in a Teflon tube), leading to the same result with only a 1% deviation between the values. However, the Cm isotope we used was mainly 244 as opposed to the 248 isotope in the previous literature.

An issue with discussing radiolysis and formation of radical species in solution as the cause of deviations is that it does not appear to hold consistently across all cation cases. Specific activities of actinide(III) ions calculated from isotopic compositions and concentrations ( $\text{Pu}^{3+}$ : 2431 GBq/L;  $\text{Am}^{3+}$ : 3060 GBq/L;  $\text{Cm}^{3+}$ : 488 GBq/L;  $\text{Cf}^{3+}$ : 27 GBq/L) do not display correlation with magnetic susceptibility deviations from free-ion calculations. That is particularly noticeable comparing Pu(III) and Cf(III) cases. In the Evans method all actinide(III) solutions we prepared exhibited similar order of magnitude chemical shift variations, but Cm(III) and Cf(III) exhibited this at about 1 mM concentrations, while the other ions exhibit similar shifts only at concentrations around 50 mM (see Table 1). Under these conditions, we can assume the more dilute solutions may be more sensitive to small amounts of paramagnetic contaminants, despite particular attention having been paid to sample purification and preparation of Cm(III) and Cf(III).

To check whether radiolysis products have an effect on BMS measurements it would be interesting to run dedicated experiments comparing Am-241 and Am-243 isotope. Because of its weak paramagnetic behavior, Am(III) is one of the most suitable actinide to detect even small effects arising from radiolysis in aqueous solution.

**Oxidation State Four.** All the tetravalent actinide cations have experimental effective magnetic moments lower than those calculated from Hund's rule (dotted line, Supporting Information, Figure S7 and Figure 5), using their formal  $5f^2$  to  $5f^4$  electronic configurations. Hund's rule states that the electronic configuration of lowest energy and the addition of any other electronic state (through the use of the Van Vleck equation) would give rise to higher values, not lower values,

unless ligand-field effects change the ground-state level of the free-ion model.

Calvin et al.<sup>19</sup> in 1948 reported tetravalent actinide magnetic susceptibilities in chloride and sulfate solutions. They found that  $5f^2$  electronic configurations and Russell–Saunders approximation fit their results even though they obtained lower values (20% less than expected). The authors' conclusion considered several other factors, including  $5f^2 6d^1$  electronic configuration and  $j$ – $j$  coupling, and ultimately accounted for these low values as a result of the “Stark Effect” produced by electric fields of ions and water dipoles (ligand-field splitting). Despite using different experimental apparatus, our experimental results are close to these pioneer values ( $46.37 \times 10^{-9} \text{ m}^3/\text{mol}$  in  $\text{HCl } 0.5 \text{ mol L}^{-1}$ ,  $50.27 \times 10^{-9} \text{ m}^3/\text{mol}$  in  $\text{HSO}_4^- 0.2 \text{ mol L}^{-1}$ , and  $20.23 \times 10^{-9} \text{ m}^3/\text{mol}$  in  $\text{HSO}_4^- 0.5 \text{ mol L}^{-1}$  for U(IV), Np(IV), and Pu(IV)), respectively, and more importantly are still low compared to magnetic susceptibilities calculated from Hund's rule.

Recently, Danilo et al.<sup>49</sup> attempted to explain NMR relaxivities and optical spectroscopic data for  $\text{U}^{4+}$  considering a ligand-field contribution of the first hydration sphere in electronic structure calculations. The authors modeled uranium solvation with eight discrete water molecules and a continuum model describing the remaining solvent. Their techniques employed relativistic wave functions to calculate the spin–orbit contributions. They pointed out the ligand field induced by the eight water molecules in the first hydration sphere of  $\text{U}^{4+}$  raises the atomic level energy degeneracies by up to  $5700 \text{ cm}^{-1}$ , while bulk solvent effects were found to be relatively unimportant, with no difference larger than  $100 \text{ cm}^{-1}$  observed. Consequently, the hydrated  $\text{U}^{4+}$  ground state ( $^3\text{H}_4$ ) splits into 7 to 9 levels depending on extended solvation effects beyond the first coordination sphere. The ground-state splitting spans  $1446 \text{ cm}^{-1}$ , but no mixing of states that could lead to a lower energy is discussed. The authors also indicated that uranium open-shell orbitals have a strong atomic character and do not mix with the orbitals of the bonded water molecule. They reported that 1.98 unpaired electrons from Mulliken spin population analysis are localized on the uranium atom. That leaves 1% of the  $5f^2$  electrons to mix with water–ligand orbitals. This amount is low but could explain a decrease in the orbital angular momentum of the ground state  $m_l = 5$  due to the presence of water orbitals. This phenomenon, which is known as the “Stevens's orbital reduction,”<sup>50</sup> has been applied to 4d and 5d elements but also to Np(VI)<sup>11,43</sup> to explain magnetic properties. This can be interpreted to indicate a certain amount of covalent bonding with orbitals located on atoms next to the actinide(IV) ion. Quantum numbers of maximum multiplicity describing the ground state are still used in eqs 9 and 7 for magnetic susceptibility and effective magnetic moment calculation, respectively, but  $L$  is replaced by  $kL$  where  $k$  is the orbital reduction factor. Hence one finds  $k = 0.921, 0.884, \text{ and } 0.935$  for U(IV), Np(IV), and Pu(IV), respectively, to fit our experimental data Table 2. Usually, the value of  $k$  is expected to be greater than 0.85 and is 1 when there is no reduction.<sup>50</sup> The value obtained for the Np(IV) appears low compared to those of U(IV) and Pu(IV), indicating a more covalent behavior. It is apparent that finer or more comprehensive descriptions of An(IV) experimental BMS would require quantum chemistry calculations.

**Oxidation State Six.** In actinyl ions,  $5f$  orbitals participate in the An–O bonding through  $\sigma$  and  $\pi$  orbitals, leaving only two nonbonding  $5f$  orbitals ( $\delta$  and  $\phi$ ) available for unpaired electrons. The effective charge of actinyl ions is smaller than it is with actinide (IV) ions, but more importantly the charge cloud of the bonding electrons has axial symmetry around the linear O–An–O axis. These ions resemble a cylinder of charge rather than a sphere. Actinyls are molecular ions, and for this reason notation of molecular spectroscopy is usually used to assign their electronic states. Eisenstein and Pryce<sup>43,51</sup> studied the electronic structure of uranyl-like ions, considering the spin–orbit coupling to be weak in comparison with this axial field. In the case of the  $\text{NpO}_2^{2+}$  ion, which has one electron in the two available orbitals, the charge cloud repels this  $5f^1$  electron in the equatorial plane farthest away from the O–An–O axis. This electronic state of lowest energy corresponds to  $m_l = \mp 3$ . Regarding  $\text{PuO}_2^{2+}$ , which has two extra electrons in addition to the uranyl structure, Coulomb repulsion has

to be considered. Electronic paramagnetic resonance (EPR) and susceptibility experiments show that these electrons enter with parallel spins into both available states ( $\delta$  and  $\phi$ ). Eisenstein and Pryce found the ground states of uranyl, neptunyl, and plutonyl ions to be  $^1\Sigma_0$ ,  $\Phi_{\pm 5/2}$  ( $^2\Phi_{5/2}$ ), and  $^3\text{H}_4$ , respectively. Despite the strong field arising from the terminal oxo ligand, ground states of these molecular ions are finally consistent with Hund's rule. More recently, a theoretical study<sup>52</sup> performed with relativistic pseudopotential calculations for uranyl and plutonyl ions found their ground states to be  $\Sigma_0$  and  $^3\text{H}_g$ , respectively. The authors concluded the  $^3\text{H}_g$  ground state of the plutonyl can be deduced on the basis of the Hund's rules because of the atomic nature of the  $\delta$  and  $\phi$  available orbitals. This point is important because it allows the ground state of actinyl ions from the state of maximum multiplicity like normal atomic  $f$  ions and then calculation of BMS using eq 9.

Regarding U(VI), Np(VI), and Pu(VI), actinyl ions exhibit BMS or experimental effective magnetic moments (Figure 5 and Supporting Information, Figure S7) that appear to be in quite good agreement with calculated values from Hund's rule compared to the systematic An(IV) BMS deviations. However, this calculation must be considered as approximate because uranyl is experimentally not diamagnetic but is weakly paramagnetic. The equation does not take into account the second-order Zeeman effect to describe accurately the weak paramagnetic behavior of U(VI) mentioned previously<sup>43</sup>, suggesting involvement of electrons from a high  $l$  value.

The experimental Np(VI) BMS we found in perchlorate media is 20% weaker compared to that obtained from eq 9 applied to the  $5f^2$  electronic configuration of the free ion and 5% higher than Howland and Calvin's value ( $25.9 \times 10^{-9} \text{ m}^3/\text{mol}$  in  $0.5 \text{ M HSO}_4^-$ ). A weaker magnetic susceptibility value of about  $20 \times 10^{-9} \text{ m}^3/\text{mol}$  was found by Gruen and Hutchison, who succeeded in fitting magnetic susceptibility measurements of a neptunyl sodium acetate compound. Calculations they performed took into account a large spin–orbit coupling compared to the applied axial field.<sup>53</sup> They deduced a  $7700 \text{ cm}^{-1}$  separation between the highest and lowest of the states into which the ground state is split by the axial crystalline field. On the basis of EPR data of other neptunyl compounds, Eisenstein and Pryce<sup>43</sup> found good agreement with the Curie constant found by Gruen and Hutchison. For this purpose, they assumed no orbital moment reduction ( $k = 1$ ) but some crystal field effect ( $p = 0.2$ ). They demonstrated that the second-order effect, which is temperature-independent, arises more importantly from the  $^2\Phi_{7/2}$  energy configuration, the uranyl core paramagnetism, and finally from the  $^2\Delta_{3/2}$  energy configuration. Excited levels  $^2\Phi_{7/2}$  and  $^2\Delta_{3/2}$  used were at  $4225$  and  $18000 \text{ cm}^{-1}$ , respectively, from the ground state. Recent calculations<sup>54</sup> involving relativistic spin–orbit configuration interaction methods based on effective core potentials show the Np(VI) ground state has a strong mixing of  $^2\Phi_{5/2}$  and  $^2\Delta_{5/2}$  (68% and 17%, respectively).

In contrast to Np(VI), we observed that Pu(VI) BMS in perchlorate media (Table 2) is 5% higher than it is in the calculation obtained from eq 9 applied to the ground state  $^3\text{H}_4$  and about 37% higher than Calvin's value obtained at  $20^\circ\text{C}$  ( $44.48 \times 10^{-9} \text{ m}^3/\text{mol}$  in  $\text{HCl } 0.5 \text{ mol L}^{-1}$ ). Such a difference between experimental values obtained in solution is quite amazing and moreover unexplained. This experiment was performed three times from different preparations and each time resulted in the same magnetic susceptibility value. Eisenstein and Pryce<sup>51</sup> found a good agreement with Calvin's value thanks to a Steven's reduction factor fitted from EPR data on neptunyl rubidium nitrate and by taking into account up to 1% population of the first excited state  $^3\Sigma_0$ , which is  $1782 \text{ cm}^{-1}$  above the ground state ( $^3\text{H}_{\pm 4}$ ) in their calculation. They suggested the possibility of the ground state (or other pure states) to mix with a number of other states as well. Recent calculations,<sup>52</sup> performed with relativistic pseudopotential on the isolated plutonyl ion, confirmed that the  $^3\Sigma_g$  state is quite far from the ground state ( $3858 \text{ cm}^{-1}$ ). Even when five water molecules surrounding  $\text{PuO}_2^{2+}$  are taken into account in a CASPT2 approach,<sup>49</sup> the first excited state is found at  $2979 \text{ cm}^{-1}$ . There is definitively no possibility of the this excited state being populated at room temperature. Another alternative is to fit our Pu(VI) experimental



value considering second-order effects arising from mixing states of higher energies in the Van Vleck equation.

**Isoelectronic Actinide Ions.** Considering the  $5f^2$  case, that is,  $U^{4+}$ ,  $NpO_2^+$ , and  $PuO_2^{2+}$ , an interesting series arises in which the order of magnetic susceptibility is  $PuO_2^{2+} > U^{4+} > NpO_2^+$ . From an electronic point of view, the common  $^3H_4$  ground state applied in conjunction with eq 9 yields a magnetic susceptibility (or effective magnetic moment) that agrees most closely with the Pu(VI) experimental value. If the Pu(VI) value is considered as a baseline, the challenge is to explain why the U(IV) value and more importantly the Np(V) value are so weak (26% and 38%, respectively). We could suggest an effect arising from ligand field induced by the -yl oxygen, but that does not explain the gap between both actinyl magnetic susceptibility values. Modeling the actinyl cation electronic configurations is a challenging and ongoing area of research, with recent reports focusing on  $NpO_2^+$  and  $PuO_2^{2+}$ <sup>52,54</sup> and some work also being done with  $U^{4+}$ <sup>49</sup> taking into account effects of the first hydration sphere and bulk solvent. Few definite conclusions from these computational studies aid in the present discussion.

## CONCLUSIONS

As could be expected, the relationship between magnetic susceptibilities or effective magnetic moments and the number of  $5f$  electrons presents a shape that looks like those of the  $4f$  counterparts or the shape predicted by the Hund's rules of maximum multiplicity. However, from a more precise point of view, actinide paramagnetic behavior displays discrepancies from this simple shape, as has already been pointed out in the literature from different materials. This Study presents a comprehensive examination of all readily accessible oxidation states of actinide ions in perchloric media to get, as much as possible, similar conditions since only the number of water molecules are presumed to change. By application of Evans method, reliable and sensitive magnetic susceptibilities have been collected at different temperatures. The temperature range span is smaller than that obtained for solid-state compounds but large enough to allow the conclusion that actinide cation magnetic susceptibility is in good agreement with a Curie-like law. Slopes obtained exhibit positive Curie constants except for Th(IV) and U(VI), which are negative and zero, respectively.

Though no definitive correlation has been found between specific activities and magnetic susceptibility deviations of An(III), it would be interesting to investigate this aspect of the chemistry in more detail. Indeed, in case of weak paramagnetic behavior the small amount of radicals formed in the bulk or solvated electrons arising from  $\alpha$  and  $\beta$  emissions from the actinide ions could account for some experimental difficulties encountered in measuring magnetic susceptibility through the Evans method.

Considering the trivalent oxidation state, the magnetic behavior of the aqueous actinide cations is in better agreement with Hund's rule predictions than is that of their lanthanide analogues, especially for Pu(III) and Am(III). This can be explained by first excited states, which are a few thousand wavenumbers above the ground states as opposed to being accessible, as in the case of Eu(III) and Sm(III). In this context, the reason that the excited states of the actinides are larger than those of the lanthanides is due to the larger spin-orbit coupling in the actinides relative to the lanthanides. If we preclude possible experimental impurities, Cf(III) paramagnetic behavior appears higher than predicted for unknown reasons.

Experimental magnetic susceptibilities (or effective magnetic moments) of actinide (IV) and (V) ions exhibit systematic deviation from Hund's rule, in contrast to the actinide (VI) ions. The An(IV) magnetic susceptibilities are found to be

lower than the value predicted by the ground state for the free ion and could be explained by covalent interactions with surrounding water molecules. Regarding An(VI) paramagnetism, there is no general trend that could explain in detail the deviations we observed from Hund's prediction and from the prior literature. In general, theoretical calculations available in the literature account well for electronic spectra and optical spectroscopy but do not provide adequate explanations for the details of actinide paramagnetic behavior.

We hope these experimental results will offer guidance for the choice of suitable cations for the study of actinide coordination chemistry/material science using NMR spectroscopy. They also provide a foundation for additional work on directed magnetism effects in actinide science.

## ASSOCIATED CONTENT

### Supporting Information

UV-vis spectra of the actinide solutions used to check cation oxidation states are presented. Wavelengths and extinction coefficients used for concentration measurements are reported with the experimental conditions. Linear regressions of actinide magnetic susceptibilities versus  $1/T$  are plotted. Results of actinide effective magnetic moments obtained at different oxidation states are also plotted and superimposed with those of the lanthanide(III) series. This material is available free of charge via the Internet at <http://pubs.acs.org>.

## AUTHOR INFORMATION

### Corresponding Authors

\*E-mail: [tfwall@wsu.edu](mailto:tfwall@wsu.edu) (T.F.W.).

\*E-mail: [claude.berthon@cea.fr](mailto:claude.berthon@cea.fr) (C.B.).

### Notes

The authors declare no competing financial interest.

## ACKNOWLEDGMENTS

T.F.W. gratefully acknowledges support from Actinet I3 (Actinide Separation Chemistry scope) and the Chateaubriand Science Fellowship 2010-2011. T.F.W. and K.N. also acknowledge support of the U.S. Department of Energy, Office of Nuclear Energy, Nuclear Energy University Programs (NEUP) Project Number 10-881. We also thank Dr. M.C. Charbonnel for her commitment in solving the administrative challenges.

## REFERENCES

- (1) Caravan, P.; Mehrkhodavandi, P.; Orvig, C. *Inorg. Chem.* **1997**, *36*, 1316–1321.
- (2) Desreux, J. F. In *Advances in Inorganic Chemistry*; van Eldik, R., Bertini, I., Eds.; Elsevier Science: New York, 2005; Vol. 57; pp 381–403.
- (3) Jackson, J. A.; Lemons, J. F.; Taube, H. J. *Chem. Phys.* **1960**, *32*, 553–555.
- (4) Lewis, W. B.; Jackson, J. A.; Lemons, J. F.; Taube, H. J. *Chem. Phys.* **1962**, *36*, 694–701.
- (5) Djanashvili, K.; Peters, J. A. *Contrast Media Mol. Imaging* **2007**, *2*, 67–71.
- (6) Swift, T. J.; Connick, R. E. *J. Chem. Phys.* **1962**, *37*, 307–320.
- (7) Swift, T. J.; Connick, R. E. *J. Chem. Phys.* **1964**, *41*, 2553–2554.
- (8) Helm, L.; Nicolle, G. M.; Merbach, A. E. In *Advances in Inorganic Chemistry*; van Eldik, R., Bertini, I., Eds.; Elsevier Science: New York, 2005; Vol. 57; pp 327–379.
- (9) Wall, T. F.; Nash, K.; Charbonnel, M. C.; Guerin, L.; Berthon, C. NUCL-104: Coordination Study of Pu(III) and Pu(VI) by NMR. In *Abstracts of Papers*, 242nd ACS National Meeting and Exposition,

Denver, CO, Aug 28–Sept 1, 2011; American Chemical Society: Washington, DC, 2011

- (10) Walstedt, R. E.; Kambe, S.; Tokunaga, Y.; Sakai, H. *J. Phys. Soc. Jpn.* **2007**, *76*, 1–17.
- (11) Bleaney, B. *Discuss. Faraday Soc.* **1955**, *19*, 112–118.
- (12) Fournier, J. M. *Ann. Phys.* **1971**, 159–166.
- (13) Fournier, J. M. *J. Phys. (Paris)* **1972**, *33*, 699–706.
- (14) Huray, P. G.; Nave, S. E.; Haire, R. G. *J. Less-Common Met.* **1983**, *93*, 293–300.
- (15) Dawson, J. K. *Nucleonics* **1952**, *10*, 39–45.
- (16) Nave, S. E.; Haire, R. G.; Huray, P. G. *Phys. Rev. B: Condens. Matter Mater. Phys.* **1983**, *28*, 2317–2327.
- (17) Lawrence, R. W. *J. Am. Chem. Soc.* **1934**, *56*, 776–783.
- (18) Calvin, M. *Plutonium Project Report CK-2411*; 1944.
- (19) Calvin; Kasha; Sheline, *AECD-2002*; 1948.
- (20) Hutchinson, C. A.; Elliott, N. *AECD-1896*; 1948.
- (21) Howland, J. J.; Calvin, M. *J. Chem. Phys.* **1950**, *18*, 239–243.
- (22) Lewis, G. N.; Calvin, M. *J. Am. Chem. Soc.* **1945**, *67*, 1232.
- (23) Theorell, H. *Ark. Kemi, Mineral Geol.* **1943**, 16A.
- (24) Evans, D. F. *J. Chem. Soc.* **1959**, 2003–2005.
- (25) Deutsch, J. L.; Poling, S. M. *J. Chem. Educ.* **1969**, *46*, 167–168.
- (26) Loliger, J.; Scheffold, R. *J. Chem. Educ.* **1972**, *49*, 646–647.
- (27) Engel, R.; Halpern, D.; Bienenfeld, S. *Anal. Chem.* **1973**, *45*, 367–369.
- (28) Grant, D. H. *J. Chem. Educ.* **1995**, *72*, 39–40.
- (29) Piguet, C. *J. Chem. Educ.* **1997**, *74*, 815–816.
- (30) De Buysser, K.; Herman, G. G.; Bruneel, E.; Hoste, S.; Van Driessche, I. *Chem. Phys.* **2005**, *315*, 286–292.
- (31) Berger, S.; Braun, S. *200 and More NMR Experiments*; Wiley-VCH: New York, 2004.
- (32) Berthon, C.; Delangle, P.; Moisy, P.; Charbonnel, M.-C.; Nikitenko, S. I.; Bosse, E.; Grigoriev, M. S. *IOP Conf. Series: Materials Science and Engineering* **2010**, *9*, 1–6.
- (33) Braekers, D. *Chimie des Actinides: Retraitement des Combustibles Nucléaires et Applications de la Résonance Magnétique Nucleaire*. Ph.D. Thesis, Université de Liège: Belgium, 2009.
- (34) Dupouy, G.; Bonhoure, I.; D, C. S.; Dumas, T.; C, H.; Le Naour, C.; Moisy, P.; Petit, S.; Scheinost, A.; Simoni, E.; Den Auwer, C. *Eur. J. Inorg. Chem.* **2011**, *10*, 1560–1569.
- (35) Revel, R.; Den Auwer, C.; Madic, C.; David, F.; Fourest, B.; Hubert, S.; Le Du, J. F.; Morss, L. R. *Inorg. Chem.* **1999**, *38*, 4139–4141.
- (36) Hendricks, M. E.; Jones, E. R., Jr; Stone, J. A.; Karkaker, D. G. *J. Chem. Phys.* **1974**, *60*, 2095–2103.
- (37) Takikawa, Y.; Ebisu, S.; Shoichi, N. *J. Phys. Chem. Solids* **2010**, *71*, 1592–1598.
- (38) Van Vleck, J. H. *The Theory of Electric and Magnetic Susceptibilities*; Oxford University Press: New York, 1932.
- (39) Hund, F. *Z. Phys.* **1925**, *33*, 855–859.
- (40) Apostolidis, C.; Schimmelpfennig, B.; Magnani, N.; Lindqvist-Reis, P.; Walter, O.; Sykora, R.; Morgenstern, A.; Colineau, E.; Caciuffo, R.; Klenze, R.; Haire, R. G.; Rebizant, J.; Bruchertseifer, F.; Fanghänel, T. *Angew. Chem., Int. Ed.* **2010**, *49*, 6343–6347.
- (41) Van Vleck, J. R. *Ann. Inst. Henri Poincaré* **1947**, *10*, 57–187.
- (42) Bain, G. A.; Berry, J. F. *J. Chem. Educ.* **2008**, *85*, 532–536.
- (43) Eisenstein, J. C.; Pryce, H. L. *Proc. R. Soc. Lond. A* **1955**, 229, 20–38.
- (44) Tremolét de Lacheisserie, E. et al. In *Magnétisme. Tome I, Fondements*; EDP Sciences, Ed.; EDP Sciences: France, 2000.
- (45) Soderholm, L.; Edelstein, N.; Morss, L. R.; Shalimoff, G. V. *J. Magn. Mater.* **1986**, *54–57*, 597–598.
- (46) Rabideau, S. W. *J. Am. Chem. Soc.* **1953**, *75*, 798–801.
- (47) Hessler, J. P.; Carnall, W. T. *ACS Symp. Ser.* **1980**, *131*, 349–368.
- (48) Morss, L. R.; Fuger, J.; Goffart, J.; Haire, R. G. *Inorg. Chem.* **1983**, *22*, 1993–1996.
- (49) Danilo, C.; Vallet, V.; Flament, J. P.; Wahlgren, U. *Phys. Chem. Chem. Phys.* **2010**, *12*, 1116–1130.
- (50) Stevens, K. W. H. *Proc. R. Soc. Lond., Ser. A* **1953**, *219*, 542–555.
- (51) Eisenstein, J. C.; Pryce, H. L. *Proc. R. Soc. Lond., Ser. A* **1956**, *238*, 31–45.
- (52) Ismail, N.; Heully, J. L.; Saue, T.; Daudey, J. P.; Marsden, C. J. *Chem. Phys. Lett.* **1999**, *300*, 296–302.
- (53) Gruen, D.; Hutchison, C. A. *J. Chem. Phys.* **1954**, *22*, 386–393.
- (54) Matsika, S.; Pitzer, R. M. *J. Phys. Chem. A* **2000**, *104*, 4064–4068.